Insights into the Solution Structure of Human Deoxyhemoglobin in the Absence and Presence of an Allosteric Effector†

Sarata C. Sahu,‡ Virgil Simplaceanu,‡ Qingguo Gong,‡,§ Nancy T. Ho,‡ Fang Tian,|| James H. Prestegard,|| and Chien Ho*,‡

Department of Biological Sciences, Carnegie Mellon University, Pittsburgh, Pennsylvania 15213, and Complex Carbohydrate Research Center, University of Georgia, Athens, Georgia 30602

Received May 15, 2007; Revised Manuscript Received June 29, 2007

ABSTRACT: We present a nuclear magnetic resonance (NMR) study in solution of the structures of human normal hemoglobin (Hb A) in the deoxy or unligated form in the absence and presence of an allosteric effector, inositol hexaphosphate (IHP), using $^{15}N-^{1}H$ residual dipolar coupling (RDC) measurements. There are several published crystal structures for deoxyhemoglobin A (deoxy-Hb A), and it has been reported that the functional properties of Hb A in single crystals are different from those in solution. Carbonmonoxyhemoglobin A (HbCO A) can also be crystallized in several structures. Our recent RDC studies of HbCO A in the absence and presence of IHP have shown that the solution structure of this Hb molecule is distinctly different from its classical crystal structures (R and R2). To have a better understanding of the structure−function relationship of Hb A under physiological conditions, we need to evaluate its structures in both ligated and unligated states in solution. Here, the intrinsic paramagnetic property of deoxy-Hb A has been exploited for the measurement of RDCs using the magnetic-field dependence of the apparent one-bond $^{1}H-^{15}N$ *J* couplings. Our RDC analysis suggests that the quaternary and tertiary structures of deoxy-Hb A in solution differ from its recently determined high-resolution crystal structures. Upon binding of IHP, structural changes in deoxy-Hb A are also observed, and these changes are largely within the $\alpha_1\beta_1$ (or $\alpha_2\beta_2$) dimer itself. These new structural findings allow us to gain a deeper insight into the structure−function relationship of this interesting allosteric protein.

Human normal adult hemoglobin (Hb A),[1] a heterotetrameric protein that transports oxygen from the lungs to tissues, has served as an excellent model for investigating the structure−function relationship in multimeric, allosteric proteins. Hb A consists of four subunits, i.e., two identical α-chains of 141 amino acid residues each and two identical β-chains of 146 amino acid residues each; each subunit contains a heme group leading to a complex with a molecular weight of ∼ 64 500. The heme iron atom undergoes a spin-state change in going from a high-spin paramagnetic Fe^{+2} ($S = 2$) in the deoxy or unligated form to a diamagnetic Fe^{2+} ($S = 0$) in the ligated form (with O_2 or CO). The oxygenation of Hb A is regulated by interactions between the O_2-binding sites (homotropic interactions) and interactions between individual amino acid residues in the protein molecule and various solutes (heterotropic interactions). Heterotropic effectors include hydrogen ions, chloride ions, carbon dioxide, inorganic phosphate ions, and organic phosphate ions [e.g., 2,3-bisphosphoglycerate (2,3-BPG) and inositol hexaphosphate (IHP)] and are known to modulate the oxygen affinity of hemoglobin. For reviews on the structure−function relationship on hemoglobin, see refs *1*−*3*. Allosteric effectors 2,3-BPG and IHP exert a significant effect on the oxygen-binding properties of Hb A. Arnone (*4*) reported that 2,3-BPG binds to the central cavity of the Hb molecule in the deoxy form, specifically to βVal1, βHis2, βLys82, and βHis143, and thus stabilizes the deoxy quaternary structure and lowers the oxygen affinity. Arnone and Perutz (*5*) reported that IHP also binds to the central cavity of the deoxy-Hb A molecule, specifically at amino residues βHis2, βLys82, βAsp139, and βHis143. According to Arnone and co-workers (*6*), IHP is disordered in the low-salt quaternary-T crystals, and therefore, they have not modeled the IHP molecule in its β−β binding site. Yonetani et al. (*7*) reported that allosteric effectors, such as 2,3-BPG, bezafibrate (BZF), and IHP, affect the ligation-linked tertiary structural changes rather than the homotropic ligation-linked T/R quaternary structural transition. Recently, we have reported that IHP alters both the tertiary and the quaternary structures of HbCO A (*8*). It appears that the role of allosteric effectors in the structure−function relationship of Hb A is not fully understood.

† This work is supported by research grants from the National Institutes of Health (R01HL-024525 and S10RR-017815 to C.H. and P41GM066340 to J.H.P.).

* To whom correspondence should be addressed. Phone: (412) 268-3395. Fax: (412) 268-7083. E-mail: chienho@andrew.cmu.edu.

‡ Carnegie Mellon University.

§ Present address: Department of Structural Biology, School of Medicine, University of Pittsburgh, Pittsburgh, PA 15261.

|| University of Georgia.

[1] Abbreviations: Hb A, human normal adult hemoglobin; HbCO, carbonmonoxyhemoglobin; deoxy-Hb, deoxyhemoglobin; 2,3-BPG, 2,3-bisphosphoglycerate; IHP, inositol hexaphosphate; NMR, nuclear magnetic resonance; RDC, residual dipolar coupling; RMSD, root-mean-square deviation; χ^2, chi squared; HSQC, heteronuclear single-quantum coherence; TROSY, transverse relaxation-optimized spectroscopy; PDB, Protein Data Bank; SVD, singular value decomposition.

10.1021/bi700935z CCC: $37.00
Published on Web 08/11/2007

Our current understanding of hemoglobin function rests largely on the crystallographic structures of ligated and unligated hemoglobin proposed by Perutz and co-workers (*9*, *10*), who identified two quaternary conformations of this protein, commonly known as the R and T states of the Monod−Wyman−Changeux (MWC) model of cooperativity (*11*). In the simplest description of this model, the protein switches between a tense (T), low-affinity state in the unligated form, and a relaxed (R), high-affinity state upon ligand binding. A new quaternary structure in the ligated state, R2, was observed by Silva et al. (*12*). By a comparison of the geometric coordinates of the T, R, and R2 structures, Srinivasan and Rose (*13*) concluded that, in the transition from the unligated deoxy form to the ligated form, the quaternary structure shifts from T to R and then to R2; i.e., R is the intermediate state (*13*). More recently, two additional X-ray crystal structures termed R3 and RR2 have been found in the family of ligated Hb A structures by Safo and Abraham (*14*). Thus, HbCO A exhibits a large number of R-type crystal structures, differing in structural detail, depending on a number of factors including the crystallization conditions. There are also several X-ray crystallographic structures for deoxy-Hb A available in the Protein Data Bank [PDB accession numbers 1A3N (*15*), 4HHB (*16*), 1HGA (*17*), 1KD2 (*18*), 1RQ3 (*19*), 1XXT (*6*), 1BZ0 (*20*), 1YHR (*6*), and 2DN2 (*21*)] which were crystallized under different temperature, pH, buffer, and salt conditions.

A basic assumption in correlating protein structure and function is that the structure of a protein in the crystalline state is the same as that under physiological solution conditions. It has been assumed that the weak intermolecular forces in a highly hydrated crystal are unlikely to shift the elements of a well-ordered protein relative to those of another one. However, this does not necessarily hold true for proteins that can switch between different conformations under allosteric control. The presence of such plasticity can be frozen out in the crystalline state; this can be even more severe for the cryocooled protein crystals where the structures of the highest resolution are determined. It has also been reported that the functional properties of Hb A in crystals are different from those in solution, e.g., the absence of a Bohr effect, cooperativity, and an allosteric effector effect in the Hb crystals (*22*). Since the protein performs its physiological functions in the solution state, it is important as well as essential to investigate the structures of Hb A in solution, both in the presence and in the absence of ligands, and to compare them to the crystal structures. At present, there is no reported structure of deoxy-Hb A under solution conditions.

Our recent NMR structural studies using $^{15}N-^{1}H$ residual dipolar coupling (RDC) measurements have shown that the solution structure of HbCO A is distinctly different from the classical crystal structures (R and R2) for HbCO A. In fact, it is a dynamic ensemble between the R and R2 structures (*8*, *23*). The difference in structure between the R and R2 states is comparable in magnitude to that between the T and R states (*12*, *24*), with R2 being the farthest away from the T structure (*8*, *13*). For deoxy-Hb A, two distinct conformations with different affinities in the T state have been reported by trapping the conformations using silicate sol−gels (*25*, *26*). This has led to speculations about the possible implications of the structural differences in the T-state of deoxy-Hb A. Thus, we need to investigate the solution structure of deoxy-Hb A, and we would like to know if and what structural changes are induced by allosteric effectors.

To address these questions, we have carried out a structure investigation of deoxy-Hb A in solution in the absence and presence of IHP using the measurements of the magnetic-field-induced $^{1}H-^{15}N$ RDCs. It is now well-established that RDCs can provide direct information on the preferred orientations of various structural elements in proteins (see reviews in refs *27* and *28*). However, obtaining data under conditions where small environment-induced changes are of interest is challenging. In isotropic solution, proteins assume all possible orientations with equal probability and the direct magnetic dipolar interaction between nuclei is averaged to zero. Nonzero averages giving rise to RDCs are obtained by using liquid-crystal or phage media to partially orient proteins, but the interactions with these media can create undesirable effects (*29*, *30*). Preparation in gel or liquid-crystal media can also lead to challenges when proteins need to be protected from atmospheric oxygen or when subtle interactions with solutes are of interest. Proteins with large anisotropic magnetic susceptibilities can orient sufficiently (typically several parts per ten thousand) at high magnetic fields without the aid of liquid crystals or phages. In the case of deoxy-Hb A, despite its symmetry, orientation can be achieved due to the large anisotropy of the paramagnetic magnetic susceptibility of the hemes in the deoxy state ($S = 2$) and interaction of the induced moments with high magnetic fields as described previously (*31*). In the present study, we have extended our initial studies of the magnetic-field-induced RDCs to investigate the solution structure of deoxy-Hb A in the absence and presence of IHP. The results shed new insights into the structure−function relationship in hemoglobin in solution.

MATERIALS AND METHODS

Sample Preparation. Two types of chain specifically U-[^{2}H,^{15}N]-labeled HbCO A samples, namely, α-chains labeled and β-chains unlabeled, and α-chains unlabeled and β-chains labeled, were prepared as described previously (*32*). The preparation of chain specifically labeled Hb samples in the deoxy form is described by Sahu et al. (*31*, *33*). NMR samples consisted of oxygen-free hemoglobin at 1 mM concentration (per tetramer) in 50 mM sodium phosphate buffer at pH 7.0. For IHP binding studies, the NMR samples were the same as above, except that the samples also contained 5 mM IHP.

NMR Spectroscopy. NMR experiments were carried out on four different high-field NMR spectrometers, Bruker DRX-500 and DRX-600 and Varian Inova-800 and Inova-900, operating at ^{1}H resonance frequencies of 500, 600, 800, and 900 MHz, respectively. All spectrometers were equipped with triple-resonance (^{1}H, ^{13}C, and ^{15}N) cryo-temperature or room-temperature probes equipped with pulsed-field gradients. The *J* couplings were measured in the ^{15}N dimension from interleaved heteronuclear single-quantum coherence (HSQC) and temperature-compensated transverse relaxation-optimized spectroscopy (TROSY) spectra (*34*, *35*). All NMR measurements, both in the absence and in the presence of IHP, were carried out at 35 °C. The sample stability was monitored by inspecting 1D ^{1}H and 2D HSQC and/or

TROSY spectra recorded before the main experiments were started and after they were completed.

RDC Analysis. If the protein is ^{15}N-labeled, each amide (^{1}H, ^{15}N) group can experience an RDC:

$$^1D_{NH} = D_a\left[(3\cos^2\theta - 1) + \frac{3}{2}R\sin^2\theta\cos 2\phi\right] \quad (1)$$

where D_a and R are the magnitude and rhombicity of the alignment tensor and the polar angles θ and ϕ describe the orientation of the NH bond vector with respect to the alignment frame (*36*). In our case, D_a, R, and the orientation of the alignment frame with respect to the molecule were determined by fitting eq 1 to a set of dipolar couplings ($^1D_{NH}$) measured for amides within a known, rigid, substructure of the protein molecule. Fitting was done using singular-value decomposition (SVD) (*37*) or nonlinear least-squares methods. Analysis included a comparison of experimental RDCs with back-calculated RDC values as described previously (*23*). Both root-mean square deviation (RMSD) and χ^2 values have been used to characterize the quality of the fit between the experimental and back-calculated RDCs. For deoxy-Hb A in the absence of IHP, the errors in the observed RDCs were calculated as described by Bax et al. (*38*) and have been described earlier (*31*). In the case of deoxy-Hb A in the presence of IHP, the error estimation has been carried out by repeating the RDC measurements twice under similar conditions. We have observed that the precision of the measurements is a little better in the latter case than the former. In both cases, the errors in the RDCs are quite small except for a very few residues, and the overall quality of the experimental RDC data in the presence and absence of IHP is very similar (see Figure 1 for errors in the experimental RDCs).

RESULTS AND DISCUSSION

The first step in the structure determination of a protein using RDCs is the backbone resonance assignment. The polypeptide backbone resonance assignments of deoxy-Hb A, required for the interpretation of the backbone RDCs, were obtained using triple-resonance TROSY-based NMR experiments applied to chain specifically labeled Hb samples (*33*). Assignment of deoxy-Hb A was a challenging task for a high-molecular-weight paramagnetic protein even after the assignment of its ligated, diamagnetic counterpart (HbCO A) was already solved (*39*). About 20% of the signals are shifted and/or severely broadened due to the presence of high-spin Fe^{2+} in the hemes of deoxy-Hb A. The presence of the hemes produces enhanced relaxation as well as causes Fermi and/or pseudocontact interactions with nearby amino acid residues and the atoms on the porphyrins. The apparent $^1D_{NH}$ values were determined from the B_0^2 dependence of the one-bond ^{15}N$-^1$H splittings ($^1J_{NH} + {}^1D_{NH}$), measured for deoxy-Hb A samples at four different magnetic fields (11.7, 14.1, 19.8, and 21.1 T). The field-induced RDCs are most apparent at the highest magnetic field used (900 MHz ^{1}H frequency or 21.1 T) as described previously (*31*). Table 1 summarizes the ^{1}H$-^{15}$N RDCs for the $\alpha_1\beta_1$ dimer of deoxy-Hb A in the absence and presence of IHP in 50 mM sodium phosphate buffer at pH 7.0 and 35 °C. The reported RDCs are taken from measurements obtained at 21.1 T.

The peaks in HSQC and TROSY spectra of deoxy-Hb A appear to be better resolved than in the corresponding spectra of HbCO A. This is not simply the result of reduced peak widths, but is also the result of reduced crowding due to the absence of peaks in deoxy-Hb A spectra for residues whose amide NH groups are close (within ~11 Å) to the paramagnetic Fe atom of the heme. RDCs used to fit eq 1 are restricted to those peaks that are well resolved in the HSQC spectrum and correspond to amino acid residues located in the α-helical regions of the protein molecule. This selection, along with the missing peaks for groups close to the paramagnetic heme, results in a set of 69 RDCs for the $\alpha\beta$ dimer, 28 in the α-chain and 41 in the β-chain. These are sufficient in number to allow evaluation of various structural models.

All published crystal structures of Hb A exhibit *C*2 symmetry. It is primarily the orientation of the $\alpha_1\beta_1$ dimer relative to the $\alpha_2\beta_2$ dimer, i.e., the orientation of the *C*2 axis relative to $\alpha_1\beta_1$ that varies between the T and R states. The *C*2 symmetry of deoxy-Hb A in solution is indicated by a single set of NMR backbone resonances for the two α- and the two β-chains, respectively. The $\alpha_1\beta_1$ backbone coordinates of the well-defined helical structure segments superimpose relatively well between different unligated, T-state structures or between ligated, R-state structures (R and R2) separately. The deoxy-Hb A structure does not superimpose well with the HbCO A structure (Table 2). The RMSD values between the four selected X-ray structures of Hb A (two for deoxy-Hb A and two for HbCO A) when the well-defined helical segments are superimposed are shown in a matrix form in Table 2. We have used two recent T-state structures for deoxy-Hb A and the R and R2 structures for HbCO A. This comparison can indicate that there are subtle differences at the tertiary structure level between deoxy-Hb A and HbCO A. In other words, the tertiary structures of T- and R-states of Hb A's are slightly different. As our preliminary results have shown (*31*), the crystal structure of deoxy-Hb A, 1XXT, gives the best fit to our measured RDCs. However, the quality of the fit is still not as good as that obtained in our previous work on HbCO A in the stretched gel (*8*). This is significant considering that HSQC and TROSY spectra with better quality and resolvability have been collected for deoxy-Hb A. For 1XXT, the $\alpha_1\beta_1$ dimer itself produces a little better fit to the measured RDCs (RMSD = 1.79 Hz) than does the full tetramer (RMSD = 1.92 Hz) (see Table 4). The small difference in the quality of the fit for the dimer and tetramer of deoxy-Hb A could be due to small quaternary structure changes in the solution structure of deoxy-Hb A. However, the overall lower quality than expected implies that some of the disagreement between measured and calculated RDCs could arise from tertiary structure changes in the α- and/or β-chains of deoxy-Hb A in solution.

It has been reported that IHP binds to the central cavity of Hb A (*5*) and that the central cavity in deoxy-Hb A is larger than in HbCO A (*9*). Allosteric effectors are known to bind much tighter in deoxy-Hb than in ligated Hb (*1*). Also, there are reports of multiple binding sites for IHP in HbCO A (*40*, *41*). All of this could lead to more extensive tertiary structure changes in the deoxy-Hb. We describe our investigation of the structural differences observed in the

Table 1: $^{1}H-^{15}N$ RDC Values for the $\alpha_1\beta_1$ Dimer of Deoxy-Hb A in the Absence and Presence of IHP in 50 mM Sodium Phosphate Buffer at pH 7.0 and 35 °C[a]

residue no.	residue name	chain ID	RDC (Hz) −IHP	RDC (Hz) +IHP	residue no.	residue name	chain ID	RDC (Hz) −IHP	RDC (Hz) +IHP
6	Asp	α_1	−1.57 ± 0.18	−2.84 ± 0.11	165	Gly	β_1	4.02 ± 0.31	2.57 ± 0.16
14	Trp	α_1	−4.71 ± 0.31	−5.01 ± 0.20	166	Gly	β_1	5.61 ± 0.33	4.55 ± 0.16
16	Lys	α_1	−5.46 ± 0.17	−5.43 ± 0.10	171	Arg	β_1	−1.20 ± 0.41	−1.24 ± 0.20
23	Glu	α_1	3.86 ± 0.33	2.21 ± 0.08	172	Leu	β_1	1.18 ± 1.16	−3.24 ± 0.89
26	Ala	α_1	1.66 ± 0.24	1.78 ± 0.16	173	Leu	β_1	7.04 ± 2.25	7.60 ± 2.42
30	Glu	α_1	0.54 ± 0.45	0.94 ± 0.23	176	Tyr	β_1	3.97 ± 0.43	1.85 ± 0.36
39	Thr	α_1	5.10 ± 0.65	5.51 ± 0.12	181	Arg	β_1	−4.36 ± 0.44	−4.03 ± 0.25
41	Thr	α_1	−9.72 ± 1.03	−8.98 ± 0.17	183	Phe	β_1	−4.93 ± 0.87	−5.31 ± 0.94
45	His	α_1	−4.89 ± 0.30	−5.26 ± 0.29	186	Phe	β_1	7.44 ± 0.27	3.28 ± 0.19
46	Phe	α_1	−5.44 ± 0.15	−5.52 ± 0.14	187	Gly	β_1	5.72 ± 0.11	4.78 ± 0.09
47	Asp	α_1	−3.52 ± 0.12	−4.03 ± 0.10	191	Thr	β_1	−3.01 ± 0.11	−3.25 ± 0.12
57	Gly	α_1	−5.68 ± 1.21	−3.85 ± 0.05	195	Val	β_1	−3.63 ± 0.13	−3.91 ± 0.14
73	Val	α_1	6.63 ± 0.13	6.49 ± 0.07	197	Gly	β_1	−2.81 ± 0.23	−4.74 ± 0.11
76	Met	α_1	−4.05 ± 0.11	−3.79 ± 0.06	198	Asn	β_1	3.30 ± 0.18	3.53 ± 0.11
81	Ser	α_1	0.44 ± 0.35	0.08 ± 0.09	202	Lys	β_1	−1.44 ± 0.22	−6.00 ± 0.15
89	His	α_1	1.44 ± 0.44	1.44 ± 0.44	203	Ala	β_1	−5.25 ± 0.30	−5.67 ± 0.32
96	Val	α_1	7.30 ± 1.87	8.02 ± 0.14	213	Ser	β_1	−1.97 ± 0.56	−2.12 ± 0.61
100	Leu	α_1	5.79 ± 0.46	5.79 ± 0.46	215	Gly	β_1	−5.76 ± 0.37	−5.93 ± 0.17
107	Val	α_1	8.55 ± 0.43	8.84 ± 0.11	216	Leu	β_1	0.58 ± 0.19	−0.99 ± 0.11
108	Thr	α_1	8.70 ± 0.24	9.37 ± 0.11	217	Ala	β_1	−8.28 ± 0.14	−7.37 ± 0.11
110	Ala	α_1	12.90 ± 0.18	12.04 ± 0.09	219	Leu	β_1	6.13 ± 0.24	6.64 ± 0.15
112	His	α_1	6.26 ± 0.16	5.57 ± 0.09	221	Asn	β_1	8.98 ± 0.13	9.02 ± 0.09
116	Glu	α_1	−10.3 ± 0.14	−6.67 ± 0.16	225	Thr	β_1	−8.07 ± 0.33	−9.08 ± 0.18
117	Phe	α_1	−1.06 ± 0.13	−0.56 ± 0.07	226	Phe	β_1	−3.65 ± 0.25	−3.08 ± 0.15
121	Val	α_1	7.35 ± 0.17	8.69 ± 0.09	227	Ala	β_1	−4.42 ± 0.21	−4.54 ± 0.10
122	His	α_1	7.24 ± 0.15	5.48 ± 0.13	252	Val	β_1	7.78 ± 0.27	4.73 ± 0.24
129	Leu	α_1	6.10 ± 0.24	6.18 ± 0.08	268	Gln	β_1	−8.59 ± 0.19	−6.89 ± 0.11
130	Ala	α_1	5.80 ± 0.22	5.63 ± 0.15	269	Ala	β_1	−5.10 ± 0.19	−3.74 ± 0.15
152	Val	β_1	4.81 ± 0.16	4.60 ± 0.10	276	Ala	β_1	−10.1 ± 0.60	−8.70 ± 0.15
153	Thr	β_1	4.04 ± 0.20	4.36 ± 0.22	277	Gly	β_1	−4.85 ± 0.27	−5.70 ± 0.17
155	Leu	β_1	9.04 ± 0.19	8.12 ± 0.12	278	Val	β_1	−2.81 ± 0.27	−2.49 ± 0.28
157	Gly	β_1	−7.29 ± 0.30	−6.41 ± 0.18	280	Asn	β_1	−7.70 ± 0.26	−15.3 ± 0.11
158	Lys	β_1	8.44 ± 0.28	7.30 ± 0.17	283	Ala	β_1	−9.16 ± 0.32	−11.6 ± 0.20
159	Val	β_1	4.86 ± 0.20	5.25 ± 0.22	284	His	β_1	5.92 ± 0.34	7.20 ± 0.08
164	Val	β_1	−0.77 ± 0.23	−0.76 ± 0.14					

[a] The reported RDCs are taken from the measurements obtained at 21.1 T.

Table 2: RMSD Matrix (Å) between the Structured Regions in the $\alpha_1\beta_1$ Dimer of Hb A[a]

PDB ID	T (1XXT)	T (2DN2)	R (1IRD) (high salt)	R2 (1BBB) (low salt)
T (1XXT)	0.00	0.24	0.98	1.05
T (2DN2)	0.24	0.00	0.93	1.00
R (1IRD) (high salt)	0.98	0.93	0.00	0.37
R2 (1BBB) (low salt)	1.05	1.00	0.37	0.00

[a] The PDB IDs and the crystallization conditions for the T- and R-state structures are also given.

Table 3: Various High-Resolution Crystal Structures of Deoxy-Hb A Used in Our Analysis[a]

PDB ID	resolution (Å)	*R* factor	compound	ligation state
1A3N	1.8	0.171	HEM, ABCD	deoxy, T
4HHB	1.74	0.135	HEM, PO_4, ABCD	deoxy, T
1HGA	2.1	0.2	HEM, ABCD	deoxy, T
1KD2	1.87	0.198	HEM, ABCD	deoxy, T (high affinity)
1RQ3	1.91	0.167	HEM, ABCD	deoxy, T
1XXT	1.91	0.19	HEM, ABCD	deoxy, T
1BZ0	1.5	0.167	HEM, ABCD	deoxy, T
1YHR[b]	2.6	0.185	HEM, ABCD, O_2	oxy, T (high affinity)
2DN2	1.25	0.179	HEM, ABCD	deoxy, T

[a] The different names in this table are the standard PDB nomenclatures. [b] Crystallized with 10 mM IHP and 20% PEG.

presence and absence of IHP on deoxy-Hb A in the following paragraphs.

Nine different X-ray crystal structures of deoxy-Hb A, with the resolution ranging from 1.25 to 2.6 Å, have been selected to compare and identify which crystal structure is closer to that in solution. Detailed information about these structure files is provided in Table 3, and the details of the RDC fit to these eight different structures are shown in Table 4. The correlation plots between the observed and calculated RDCs, both in the absence and in the presence of IHP, based on the crystal structures 1A3N, 4HHB, 1HGA, 1KD2, 1RQ3, 1XXT, 1BZ0, 1YHR, and 2DN2 are shown in Figure 1. The scatter in these plots is in all cases larger than the estimated experimental precision (shown by error bars in the figure), and the scatter is in general larger in the presence of IHP (blue symbols) than it is in the absence of IHP (red symbols).

The fitting results are also summarized in Figure 2, where a comparison of the reduced χ^2 of the fit to the high-resolution X-ray crystal structures in the absence and presence of IHP is presented. The reduced χ^2 is defined as the χ^2 divided by the number of degrees of freedom.

The data suggest that the solution structure of the T-state hemoglobin is slightly different from all known high-resolution crystal structures available so far. As we have mentioned earlier, out of all high-resolution deoxy-Hb A structures in the Protein Data Bank, 1XXT provides the best fit to our RDC data. This result is interesting, because the highest resolution structure (2DN2) at 1.25 Å reported by

Table 4: Fitting Results Obtained from the $\alpha_1\beta_1$ Dimer and the Full Tetramer of Different Deoxy-Hb A Structures

PDB ID	IHP	χ^2(dimer)	χ^2(tetramer)	RMSD(dimer) (Hz)	RMSD(tetramer) (Hz)	D_a(dimer) (Hz)	R(dimer)	D_a(tetramer) (Hz)	R(tetramer)
1BZ0	−	88.5	95.2	2.037	2.025	5.49	0.31	5.49	0.31
	+	376.4	365.0	2.631	2.607	5.29	0.32	5.39	0.28
1HGA	−	64.9	104.5	1.890	2.241	5.37	0.33	5.37	0.39
	+	332.8	357.0	2.528	2.626	5.27	0.39	5.27	0.34
1KD2	−	109.5	88.6	2.199	2.030	5.37	0.28	5.37	0.42
	+	569.5	417.2	3.190	2.672	5.27	0.13	5.37	0.35
1RQ3	−	81.7	88.3	2.042	1.969	5.37	0.42	5.37	0.39
	+	341.4	365.5	2.511	2.523	5.27	0.46	5.27	0.33
1YHR	−	92.1	104.5	2.186	2.241	5.37	0.29	5.37	0.37
	+	358.3	422.9	2.647	2.733	5.27	0.36	5.27	0.34
4HHB	−	119.6	163.0	2.286	2.458	5.43	0.29	5.22	0.28
	+	522.5	504.9	3.168	2.943	5.19	0.03	5.24	0.31
1XXT	−	61.0	85.4	1.790	1.923	5.37	0.39	5.37	0.38
	+	325.2	309.0	2.404	2.659	5.27	0.37	5.27	0.21
2DN2	−	119.7	112.2	2.272	2.196	5.32	0.40	5.37	0.34
	+	435.0	405.6	2.732	2.704	5.12	0.37	5.27	0.33

Tame's group does not provide the best fit, emphasizing the fact that the structure in solution may be different.

The deviations of data from the crystal structures are even more significant in the presence of IHP. This suggests that there is a structure change in deoxy-Hb A upon IHP binding. This is not necessarily expected given the larger central cavity in the deoxy-Hb A. However, the crystal structure of deoxy-Hb A provided in 1XXT still gives the best match to the experimental data.

Then, we pose the next question of whether the structural changes induced by IHP are at the tertiary or quaternary structural levels or may be at both. We have fitted our measured RDCs to the $\alpha_1\beta_1$ dimer as well as to the whole tetramer using eight out of the nine crystal structures (4HHB, 1HGA, 1KD2, 1RQ3, 1XXT, 1BZ0, 1YHR, and 2DN2; see Table 4 for details). We have excluded the PDB file 1A3N because a more refined structure has been reported by the same research group (PDB ID 2DN2). The values for the

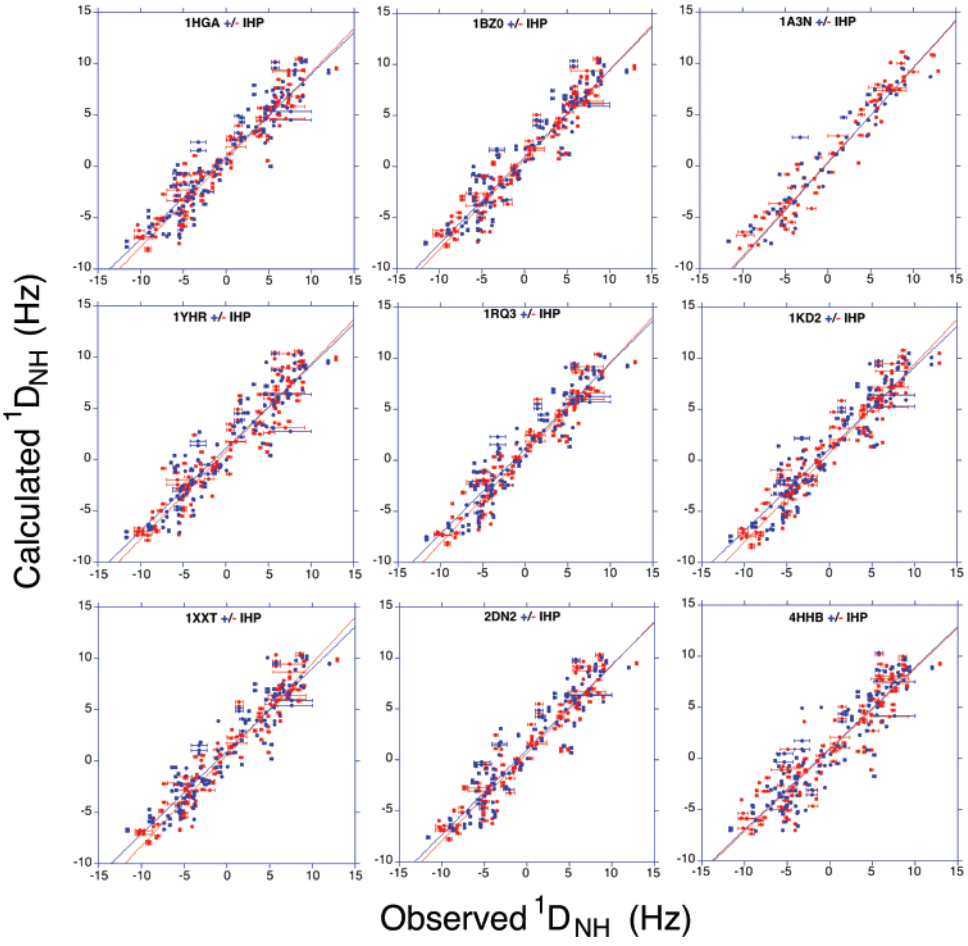

FIGURE 1: Correlation between the observed and calculated RDC values both in the presence and in the absence of IHP, based on the crystal structures 1A3N, 4HHB, 1HGA, 1KD2, 1RQ3, 1XXT, 1BZ0, 1YHR, and 2DN2 for deoxy-Hb A. For details about these PDB files, see Table 2. The data in the absence of IHP are shown in red, and those in the presence of IHP are shown in blue. Errors in the observed RDC are also shown and depicted in the same color as above.

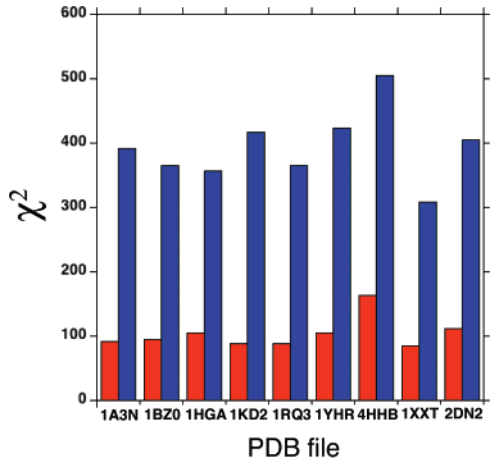

FIGURE 2: Quality of fit results from the correlation plots shown in Figure 1. The X-ray crystal structure file names are shown along the *x* axis, and their corresponding reduced χ^2 values in the absence (red) and presence (blue) of IHP are along the *y* axis.

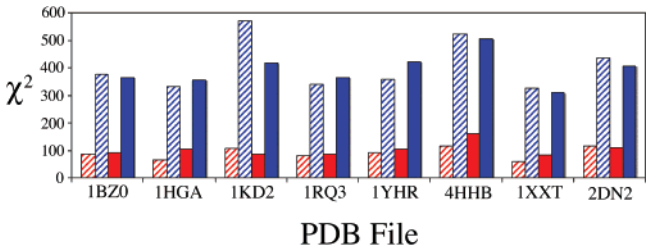

FIGURE 3: Summary of the fitting quality of our measured RDCs in the absence and presence of IHP to eight high-resolution X-ray crystal structures: 4HHB, 1HGA, 1KD2, 1RQ3, 1XXT, 1BZ0, 1YHR, and 2DN2. X-ray structure file names are shown along the *x* axis, and the corresponding reduced χ^2 values of the fit to either the $\alpha_1\beta_1$ dimer (in striped symbol) only or the whole tetramer (in filled symbol) are along the *y* axis, red color for the structure in the absence of IHP and blue color for the structure in the presence of IHP.

quality of the fit to our measured RDCs in the absence and presence of IHP with these eight high-resolution X-ray structures are summarized in Figure 3 and Table 4. The results for the $\alpha_1\beta_1$ dimer, i.e., residues 1−287, are shown as striped bars, while similar results for the entire tetramer, i.e., residues 1−574, are shown in solid color. In both the dimer and the tetramer fitting results, the data for deoxy-Hb A with and without IHP are shown in blue and red colors, respectively. The differences between the reduced χ^2 values between the dimer and tetramer fitting are very small whether we are using the data in the presence or absence of IHP. However, in either of the models (dimer or tetramer), the fit is better in the absence of IHP than in the presence of IHP. This is true regardless of the crystal structure used in the comparison. This is a clear indication of a significant change at the tertiary structure level. Analysis of the changes on an amino acid residue specific basis using just the crystal structure 1XXT is presented in Figure 4. Here the absolute differences between the observed and the calculated RDCs when fit to Hb A using the PDB structure 1XXT for different residues both in the presence and in the absence of IHP are shown. The RDCs of the sample containing IHP are shown in blue, whereas the IHP-free sample RDCs are in red. The residue numbers for the $\alpha_1\beta_1$ dimer (residues 1−287) followed by the $\alpha_2\beta_2$ dimer (residues 288−574) are shown along the *x* axis and the corresponding absolute differences

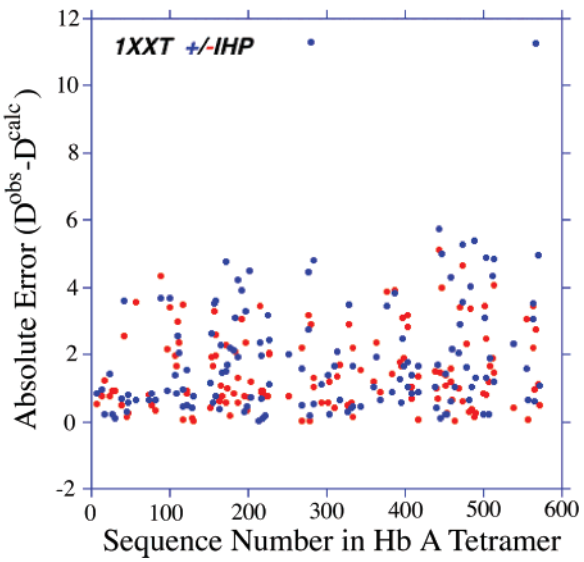

FIGURE 4: Difference (absolute value) between the observed and the calculated RDCs when fit to deoxy-Hb A using the PDB crystal structure 1XXT. The amino acid residue numbers for the $\alpha_1\beta_1$ dimer (residues 1−287) followed by the $\alpha_2\beta_2$ dimer (residues 288−574) are shown along the *x* axis and the corresponding absolute differences along the *y* axis. RDCs of the sample containing IHP are shown in blue, whereas the IHP-free sample RDCs are in red.

along the *y* axis. More residues in the β-chain undergo significant changes than in the α-chain, indicating that more residues in the β_1- and β_2-chains undergo conformational changes upon IHP binding.

Structure Change Evidenced by Chemical Shift Perturbations. Figure 5 shows representative HSQC spectra at 14.1 T of the chain specifically labeled deoxy-Hb A samples used in this work. As one can see, the addition of IHP causes a number of cross-peaks to shift, especially in the β-chain. The assignments of α-chain cross-peaks for deoxy-Hb A in the presence of IHP are very straightforward (*33*). The assignments of cross-peaks from the β-chain which undergo a significant change in peak position in HSQC spectra were confirmed by the use of 3D ^{15}N TROSY-NOESY spectra recorded at 35 °C and a 60-ms mixing time. It appears that IHP causes shifts mostly of cross-peaks from the amino acid residues located in the β-chain of deoxy-Hb A. This is in contrast to our previous work on the effect of IHP on HbCO A (*8*), where we observed chemical shift changes distributed across both α- and β-chains. However, the current findings of a larger effect of IHP on the β-chain of deoxy-Hb A are consistent with the crystallographic results on the binding of 2,3-BPG to deoxy-Hb A reported by Arnone (*4*). The differences between the CO and deoxy behavior may result from the tendency of the smaller central cavity in ligated Hb to more easily propagate changes throughout the protein molecule.

Implications of the Present Study for the Structure−Function Relationship in Hemoglobin. There are eight unique crystal structures of deoxy-Hb A that have been deposited in the Protein Data Bank with resolution ranging from 1.25 to 2.6 Å (see Figure 1 and Tables 3 and 4). The crystal structure for 1A3N has recently been refined, and the refined structure is known as 2DN2 (*21*). There are several interesting questions regarding these crystal structures. Does each of them exist as a discrete structure in solution? If so, what is the relative proportion for each of these structures in

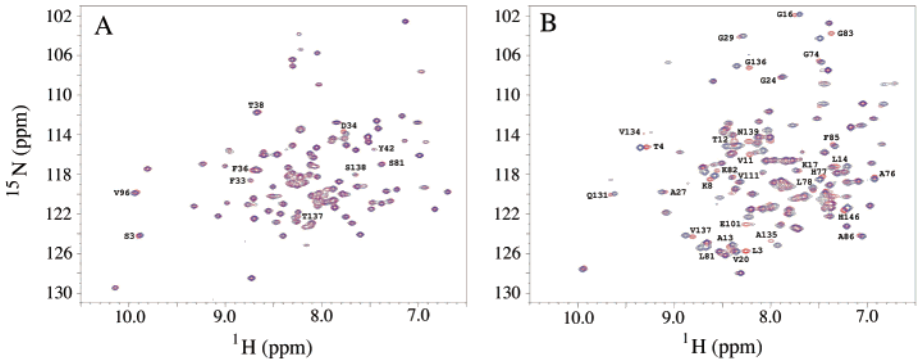

FIGURE 5: HSQC (600 MHz) (^{1}H, ^{15}N) spectra of chain specifically labeled deoxy-Hb A with IHP (blue) and without IHP (red) at 35 °C: (A) U-^{15}N,^{2}H-labeled α-chains and unlabeled β-chains; (B) unlabeled α-chains and U-^{15}N,^{2}H-labeled β-chains. In all samples, the Hb concentration was ~1 mM in 50 mM sodium phosphate at pH 7.0, and the IHP samples also contained 5 mM IHP.

solution? Does each one of them exhibit its specific functional properties? Do they interconvert among themselves, and if so, what is the time scale for this process in solution? As described in this paper, the solution structure of deoxy-Hb A as measured by the RDC method appears to be different from the nine crystal structures, with the crystal structure of 1XXT giving the best fit to our RDC data (Figure 1). Does this imply that something close to the 1XXT structure is the dominant structure for deoxy-Hb A in solution, or is the apparent structure a result of more uniform averaging of data over the representative crystal structures? With respect to the latter point, a single set of cross-peaks is observed for nearly all residues. Hence, either one structure must dominate or exchange among structures must be fast on the NMR time scale.

We can test the viability of a model in which uniform sampling of the various X-ray structures exists by using the averaging capabilities of the program REDCAT (*42*). $\alpha_1\beta_1$ dimers from seven of the unliganded X-ray structures (excluding the mutant 1YHR) were superimposed in a manner that led to overlap of the hemes in each structure, hydrogens were added to the amide sites using standard geometries, and the combined set of new coordinates was used to find the alignment parameters that best fit a model in which each of the seven structures was populated equally. The back-calculated RDCs from this model showed an RMSD relative to experiment of 1.88 Hz. This is only slightly worse than the RMSD of the 1XXT structure, and it is significantly better than the average RMSD over the set of structures, 2.07. Of course, there is no reason to expect equal sampling of the X-ray structures, and it is likely that populations could be adjusted to produce a better fit.

Recently, we have carried out model-free-based NMR dynamics studies for the polypeptide backbone amide N−H bond vectors for both the deoxy- and carbonmonoxy forms of Hb A, using ^{15}N relaxation parameters and heteronuclear nuclear Overhauser effects measured at 29 and 34 °C and at 11.7 and 14.1 T (*43*). We have found that in both deoxy and carbonmonoxy forms of Hb A, the amide N−H bonds of most amino acid residues are rigid on the fast time scale (nanoseconds to picoseconds), except for the loop regions and certain helix−helix connections. The C-terminal β146His has been postulated to play an important role in the allostery of Hb A on the basis of X-ray crystallographic data as well as its ability to form salt bridges and H-bonds in the deoxy form (*9*). Our backbone dynamics data indicate that this residue is rigid in deoxy-Hb A, but it is free from restrictions to its backbone motions in the CO form, consistent with the X-ray crystallographic findings. We have found that, in the deoxy form, α31Arg and β123Thr, neighbors in the intradimer ($\alpha_1\beta_1$) interface, exhibit stiffening upon CO binding. We have also found that there is considerable flexibility in the $\alpha_1\beta_1$ interface, e.g., B, G, and H helices and the GH corner, and that several amino acid residues (e.g., β109Val) at this interface appear to be involved in a conformational exchange process in the deoxy form. We have already reported that the solution structure of HbCO A is a dynamic ensemble of the R and R2 crystal structures (*23*). While additional research is needed to gain a deeper insight, there is sufficient information to suggest that a dynamic ensemble may exist in the deoxy form as well.

In conclusion, the plasticity and dynamic picture of hemoglobin is consistent with the emerging view of allostery as a change in the population distribution of an ensemble of structures, rather than the equilibrium of only two discrete conformations, upon binding of a ligand (*6*, *8*, *23*, *42*−*45*). Hence, to understand how hemoglobin functions as an efficient oxygen carrier in our physiological system, we need to know the structure, dynamics, and function of this protein in solution.

ACKNOWLEDGMENT

We thank Drs. David H. Maillet and Xiang-jin Song for their useful discussions and critical comments. We dedicate this paper to the memory of Dr. Jonathan A. Lukin, whose research in our laboratory in Pittsburgh formed the basis for part of the work described here.

REFERENCES

1. Dickerson, R. E., and Geis, I. (1983) *Hemoglobin: Structure, Function, Evolution, and Pathology*, Benjamin/Cummings Publishing Co., Menlo Park, CA.
2. Barrick, D., Lukin, J. A., Simplaceanu, V., and Ho, C. (2004) Nuclear magnetic resonance spectroscopy in the study of hemoglobin cooperativity, *Methods Enzymol. 379*, 28−54.
3. Lukin, J. A., and Ho, C. (2004) The structure−function relationship of hemoglobin in solution at atomic resolution, *Chem. Rev. 104*, 1219−1230.
4. Arnone, A. (1972) X-ray diffraction study of binding of 2,3-diphosphoglycerate to human deoxyhaemoglobin, *Nature 237*, 146−149.
5. Arnone, A., and Perutz, M. F. (1974) Structure of inositol hexaphosphate−human deoxyhaemoglobin complex, *Nature 249*, 34−36.

6. Kavanaugh, J. S., Rogers, P. H., and Arnone, A. (2005) Crystallographic evidence for a new ensemble of ligand-induced allosteric transitions in hemoglobin: the T-to-T(high) quaternary transitions, *Biochemistry 44*, 6101−6121.
7. Yonetani, T., Park, S. I., Tsuneshige, A., Imai, K., and Kanaori, K. (2002) Global allostery model of hemoglobin. Modulation of O_2 affinity, cooperativity, and Bohr effect by heterotropic allosteric effectors, *J. Biol. Chem. 277*, 34508−34520.
8. Gong, Q., Simplaceanu, V., Lukin, J. A., Giovannelli, J. L., Ho, N. T., and Ho, C. (2006) Quaternary structure of carbonmonoxyhemoglobins in solution: structural changes induced by the allosteric effector inositol hexaphosphate, *Biochemistry 45*, 5140−5148.
9. Perutz, M. F. (1970) Stereochemistry of cooperative effects in haemoglobin, *Nature 228*, 726−739.
10. Perutz, M. F., Wilkinson, A. J., Paoli, M., and Dodson, G. G. (1998) The stereochemical mechanism of the cooperative effects in hemoglobin revisited, *Annu. Rev. Biophys Biomol. Struct. 27*, 1−34.
11. Monod, J., Wyman, J., and Changeux, J. P. (1965) On the nature of allosteric transitions: a plausible model, *J. Mol. Biol. 12*, 88−118.
12. Silva, M. M., Rogers, P. H., and Arnone, A. (1992) A third quaternary structure of human hemoglobin A at 1.7-A resolution, *J. Biol. Chem. 267*, 17248−17256.
13. Srinivasan, R., and Rose, G. D. (1994) The T-to-R transformation in hemoglobin: a reevaluation, *Proc. Natl. Acad. Sci. U.S.A. 91*, 11113−11117.
14. Safo, M. K., and Abraham, D. J. (2005) The enigma of the liganded hemoglobin end state: a novel quaternary structure of human carbonmonoxy hemoglobin, *Biochemistry 44*, 8347−8359.
15. Tame, J. R., and Vallone, B. (2000) The structures of deoxy human haemoglobin and the mutant Hb Tyralpha42His at 120 K, *Acta Crystallogr., D: Biol. Crystallogr. 56*, 805−811.
16. Fermi, G., Perutz, M. F., Shaanan, B., and Fourme, R. (1984) The crystal structure of human deoxyhaemoglobin at 1.74 A resolution, *J. Mol. Biol. 175*, 159−174.
17. Liddington, R., Derewenda, Z., Dodson, E., Hubbard, R., and Dodson, G. (1992) High resolution crystal structures and comparisons of T-state deoxyhaemoglobin and two liganded T-state haemoglobins: T(alpha-oxy)haemoglobin and T(met)haemoglobin, *J. Mol. Biol. 228*, 551−579.
18. Seixas, F. A., de Azevedo, W. F., Jr., and Colombo, M. F. (1999) Crystallization and x-ray diffraction data analysis of human deoxyhaemoglobin A(0) fully stripped of any anions, *Acta Crystallogr., D: Biol. Crystallogr. 55*, 1914−1916.
19. Chan, N. L., Kavanaugh, J. S., Rogers, P. H., and Arnone, A. (2004) Crystallographic analysis of the interaction of nitric oxide with quaternary-T human hemoglobin, *Biochemistry 43*, 118−132.
20. Kavanaugh, J. S., Moo-Penn, W. F., and Arnone, A. (1993) Accommodation of insertions in helices: the mutation in hemoglobin Catonsville (Pro 37 alpha-Glu-Thr 38 alpha) generates a 3(10)→alpha bulge, *Biochemistry 32*, 2509−2513.
21. Park, S. Y., Yokoyama, T., Shibayama, N., Shiro, Y., and Tame, J. R. (2006) 1.25 A resolution crystal structures of human haemoglobin in the oxy, deoxy and carbonmonoxy forms, *J. Mol. Biol. 360*, 690−701.
22. Eaton, W. A., Henry, E. R., Hofrichter, J., and Mozzarelli, A. (1999) Is cooperative oxygen binding by hemoglobin really understood?, *Nat. Struct. Biol. 6*, 351−358.
23. Lukin, J. A., Kontaxis, G., Simplaceanu, V., Yuan, Y., Bax, A., and Ho, C. (2003) Quaternary structure of hemoglobin in solution, *Proc. Natl. Acad. Sci. U.S.A. 100*, 517−520.
24. Mueser, T. C., Rogers, P. H., and Arnone, A. (2000) Interface sliding as illustrated by the multiple quaternary structures of liganded hemoglobin, *Biochemistry 39*, 15353−15364.
25. Shibayama, N., and Saigo, S. (2001) Direct observation of two distinct affinity conformations in the T state human deoxyhemoglobin, *FEBS Lett. 492*, 50−53.
26. Samuni, U., Dantsker, D., Juszczak, L. J., Bettati, S., Ronda, L., Mozzarelli, A., and Friedman, J. M. (2004) Spectroscopic and functional characterization of T state hemoglobin conformations encapsulated in silica gels, *Biochemistry 43*, 13674−13682.
27. Prestegard, J. H., al-Hashimi, H. M., and Tolman, J. R. (2000) NMR structures of biomolecules using field oriented media and residual dipolar couplings, *Q. Rev. Biophys. 33*, 371−424.
28. Bax, A., and Grishaev, A. (2005) Weak alignment NMR: a hawk-eyed view of biomolecular structure, *Curr. Opin. Struct. Biol. 15*, 563−570.
29. Meiler, J., Prompers, J. J., Peti, W., Griesinger, C., and Bruschweiler, R. (2001) Model-free approach to the dynamic interpretation of residual dipolar couplings in globular proteins, *J. Am. Chem. Soc. 123*, 6098−6107.
30. Hus, J. C., Peti, W., Griesinger, C., and Bruschweiler, R. (2003) Self-consistency analysis of dipolar couplings in multiple alignments of ubiquitin, *J. Am. Chem. Soc. 125*, 5596−5597.
31. Sahu, S. C., Simplaceanu, V., Gong, Q., Ho, N. T., Glushka, J. G., Prestegard, J. H., and Ho, C. (2006) Orientation of deoxyhemoglobin at high magnetic fields: Structural insights from RDCs in solution, *J. Am. Chem. Soc. 128*, 6290−6291.
32. Simplaceanu, V., Lukin, J. A., Fang, T. Y., Zou, M., Ho, N. T., and Ho, C. (2000) Chain-selective isotopic labeling for NMR studies of large multimeric proteins: application to hemoglobin, *Biophys. J. 79*, 1146−1154.
33. Sahu, S. C., Simplaceanu, V., Ho, N. T., Giovannelli, J. L., and Ho, C. (2006) Backbone resonance assignment of human adult hemoglobin in the deoxy form, *J. Biomol. NMR* 36 1.
34. Pervushin, K., Riek, R., Wider, G., and Wüthrich, K. (1997) Attenuated T2 relaxation by mutual cancellation of dipole-dipole coupling and chemical shift anisotropy indicates an avenue to NMR structures of very large biological macromolecules in solution, *Proc. Natl. Acad. Sci. U.S.A. 94*, 12366−12371.
35. Kontaxis, G., Clore, G. M., and Bax, A. (2000) Evaluation of cross-correlation effects and measurement of one-bond couplings in proteins with short transverse relaxation times, *J. Magn. Reson. 143*, 184−196.
36. Tjandra, N., and Bax, A. (1997) Direct measurement of distances and angles in biomolecules by NMR in a dilute liquid crystalline medium, *Science 278*, 1111−1114.
37. Losonczi, J. A., Andrec, M., Fischer, M. W., and Prestegard, J. H. (1999) Order matrix analysis of residual dipolar couplings using singular value decomposition, *J. Magn. Reson. 138*, 334−342.
38. Bax, A., Kontaxis, G., and Tjandra, N. (2001) Dipolar couplings in macromolecular structure determination, *Methods Enzymol. 339*, 127−174.
39. Lukin, J. A., Kontaxis, G., Simplaceanu, V., Yuan, Y., Bax, A., and Ho, C. (2004) Backbone resonance assignments of human adult hemoglobin in the carbonmonoxy form, *J. Biomol. NMR 28*, 203−204.
40. Zuiderweg, E. R., Hamers, L. F., de Bruin, S. H., and Hilbers, C. W. (1981) Equilibrium aspects of the binding of myo-inositol hexakisphosphate to human hemoglobin as studied by ^{31}P NMR and pH-stat techniques, *Eur. J. Biochem. 118*, 85−94.
41. Zuiderweg, E. R., Hamers, L. F., Rollema, H. S., de Bruin, S. H., and Hilbers, C. W. (1981) ^{31}P NMR study of the kinetics of binding of myo-inositol hexakisphosphate to human hemoglobin. Observation of fast-exchange kinetics in high-affinity systems, *Eur. J. Biochem. 118*, 95−104.
42. Valafar, H., and Prestegard, J. H. (2004) REDCAT: A residual dipolar coupling analysis tool. *J. Magn. Reson. 167*, 228−241.
43. Song, X., Yuan, Y., Simplaceanu, V., Sahu, S. C., Ho, N. T., and Ho, C. (2007) A comparative NMR study of the backbone dynamics of hemoglobin in the deoxy and carbonmonoxy forms, *Biochemistry 46*, 6795−6803.
44. Gunasekaran, K., Ma, B., and Nussinov, R. (2004) Is allostery an intrinsic property of all dynamic proteins? *Proteins 57*, 433−443.
45. Kern, D., and Zuiderweg, E. R. (2003) The role of dynamics in allosteric regulation, *Curr. Opin. Struct. Biol. 13*, 748−757.

BI700935Z